Constrained Multibeam Optimization for Joint Communication and Radio Sensing

Yuyue Luo*†, J. Andrew Zhang†, Wei Ni#, Jin Pan*, Xiaojing Huang†
*School of Electronic Science and Engineering, University of Electronic Science and Technology of China, China
†School of Electrical and Data Engineering, University of Technology Sydney, Australia
Data61, Commonwealth Scientific and Industrial Research Organisation, Sydney, Australia
Email: Yuyue.Luo@student.uts.edu.au; {Andrew.Zhang; Xiaojing.Huang}@uts.edu.au;
Wei.Ni@data61.csiro.au, panjin@uestc.edu.cn

***Abstract*—Multibeam technology has recently been proposed for joint communication and radio sensing (JCAS) in millimeter wave systems using analog antenna arrays. Generation of the multibeam satisfying both communication and sensing requirements is yet to be developed. In this paper, we develop closed-form solutions for optimizing the coefficient that combines communication and sensing subbeams to generate a multibeam. Our solutions maximize the received signal power for communication, in the cases (1) without constraint on sensing beamforming (BF) waveform, (2) with minimum BF gain constraints on discrete sensing directions, and (3) with a minimum total power constraint on a range of sensing directions. Simulation results are provided and validate the effectiveness of the proposed solutions.**

I. Introduction

Joint communication and radio sensing (JCAS, also known as Radar-Communications) [1], [2] integrates radio communication and sensing into one system and shares the same transmitted signals. A JCAS system has appealing features such as low-cost, resource-saving, reduced size and weight, and mutual sharing of information for improved communication and sensing performance [3]. JCAS is particularly promising for millimeter wave (mmWave) systems which have potentially high temporal and spatial resolution resulting from the large bandwidth and the use of large number of antennas due to small antenna profiles [4]. There are critical challenges, which are specific for mmWave JCAS systems, associated with the usage of beamforming (BF). To reduce hardware cost, BF in mmWave systems is typically realized by using analog antenna arrays or hybrid arrays [5]. The primary challenge for BF in JCAS is that communication and sensing have different requirements for BF. Radio sensing often requires time-varying directional scanning beams, while a stable and accurately-pointing beam is in demand for communication.

BF design for JCAS systems has been investigated in [6]–[10]. Beams with multiple mainlobes can be generated to support communication and sensing in different directions [9], [10]. Unfortunately, these problem formulations are based on digital multiple-input-multiple-output MIMO systems and are not suitable for a cost-effective analog antenna array where there are much lower degrees of freedom in optimization due to a single RF chain of the array. For JCAS with analog BF, most studies such as [6]–[8] only consider a single beam for communication and sensing, hence sensing is restricted to the communication direction. In [4], multibeam technology is introduced for mmWave JCAS, with the use of analog antenna arrays. In that work, multibeam is defined as a BF waveform with two or more mainlobes (also called subbeams) generated by a single analog array at a time. [4] provides a fixed communication subbeam along with direction-varying scanning subbeams across different packets, and is shown to be superior in balancing complexity and performance by separately generating two basic beams for communication and sensing and then combining them. However, in [4], to combine the two subbeams coherently, the proposed adaptive coefficient is not optimized.

In this paper, we improve the multibeam method in [4] by providing closed-form optimal solutions for the coefficients that combine communication and sensing subbeams. Assuming the full channel matrix $\mathbf{H}$ is known at the transmitter, we first derive the optimal combining coefficient that maximizes the received signal power without considering any constraint on the sensing waveform. We then extend the solution by considering constraints for the sensing subbeam. We consider two types of constraints: 1) the transmitter BF gain at a few discrete scanning AoDs; 2) the total scanning power at a range of directions centered on the main scanning direction. For both constraints, we provide constrained optimal solutions with low computational complexity. Simulation results validate the effectiveness of the proposed methods.

Notations: $(\cdot)^H$, $(\cdot)^*$, $(\cdot)^T$, and $(\cdot)^{-1}$ denote the Hermitian transpose, conjugate, transpose, and inverse, respectively. $|\cdot|$ and $\|\cdot\|$ denote the element-wise absolute value and the norm, respectively.

II. System Model

In this section, we briefly describe the system model, introduce the concept of multibeam technologies based on analog array, and present the principle of our multibeam optimization.

Our study on multibeam in this paper inherits from the JCAS system proposed in [4]. In the system, two nodes perform two-way point-to-point communications in the time division duplex (TDD) mode and simultaneously sensing the

This work was supported by the Foundation for Innovative Research Group of the National Natural Science Foundation of China under Grant Nos. 61721001.

environment to determine locations and speed of nearby objects. Each node uses two spatially separated analog antenna arrays, for transmission and receiving reflected sensing signals, respectively, so that self-interference can be mitigated. Only a single RF and baseband module is used and connected to the two arrays. Below we only briefly describe the essential system setup to make this paper self-contained. The readers are referred to [4] for more details of the system and the multibeam JCAS technology.

We consider M-element antenna arrays where antenna elements are equally spaced at an interval of half wavelength. We assume planar wave-front and consider a narrow-band beamforming model. The array response vector is given by

$$\mathbf{a}(\theta) = [1, e^{j\pi \sin(\theta)}, \cdots, e^{j\pi(M-1)\sin(\theta)}]^T. \tag{1}$$

A quasi-static channel model can be used for both communication and sensing, although the values of their parameters are different. Consider L-path signals with AoDs $\theta_{t,\ell}$ and AoAs $\theta_{r,\ell}$, $l = 1, \cdots, L$. For illustration convenience, we assume that transmitter and receiver arrays have the same number of antennas M. The quasi-static physical channels can then be represented as

$$\mathbf{H} = \sum_{\ell=1}^{L} b_\ell \delta(t-\tau_\ell) e^{j2\pi f_{D,\ell} t} \mathbf{a}(\theta_{r,\ell}) \mathbf{a}^T(\theta_{t,\ell}), \tag{2}$$

where for the ℓ-th path, b_ℓ is its amplitude, τ_ℓ is the propagation delay, and $f_{D,\ell}$ is the associated Doppler frequency. We consider typical multipath mmWave channels where there exists a line-of-sight (LOS) path and $(L-1)$ non-line-of-sight (NLOS) paths. The LOS path is assumed to be dominating in terms of signal power.

Let the transmitted baseband signal be $s(t)$, and the transmitter and receiver BF vectors be $\mathbf{w}_t$ and $\mathbf{w}_r$, respectively. The received signal for either sensing or communication can be written as:

$$\begin{aligned} y(t) &= \mathbf{w}_r^T \mathbf{H} \mathbf{w}_t \, s(t-\tau_\ell) + \mathbf{w}_r^T \boldsymbol{z}(t) \\ &= \sum_{\ell=1}^{L} b_\ell e^{j2\pi f_{D,\ell} t} (\mathbf{w}_r^T \mathbf{a}(\theta_{r,\ell})) (\mathbf{a}^T(\theta_{t,\ell}) \mathbf{w}_t) s(t-\tau_\ell) \\ &\quad + \mathbf{w}_r^T \boldsymbol{z}(t), \end{aligned} \tag{3}$$

where $\boldsymbol{z}(t)$ is the independently and identically distributed additive white Gaussian noise (AWGN) vector at the receiving antennas.

We want to generate a BF waveform with one subbeam (mainlobe) for communication and another one or more subbeams for sensing. The sensing subbeams need to scan areas in different directions from communication. The first method proposed in [4] uses respectively desired magnitudes for communication and sensing BF waveform (array radiation pattern), and generate two BF vectors separately. Then it combines the two BF vectors using a phase shifting term $e^{j\varphi}$ and power distribution factor ρ, as shown below

$$\mathbf{w}_t = \sqrt{\rho}\mathbf{w}_{t,c} + \sqrt{1-\rho} e^{j\varphi} \mathbf{w}_{t,s}, \tag{4}$$

where $\mathbf{w}_{t,c}$ and $\mathbf{w}_{t,s}$ are the respective BF vectors for communication and sensing, ρ $(0 < \rho < 1)$ controls the energy distribution between two BF vectors. An implicitly two-step process is applied to determine ρ and φ. The value of ρ can firstly be determined according to the mean sensing and communication distances. The value of φ is then determined to ensure coherent combination of signals from different subbeams at the communicating receiver.

By minimizing the mean squared error (MSE) between the generated BF waveform and the desired multibeam waveform with a single BF vector, the second method in [4] can generate a radiation pattern, with the shape closer to the desired one. The first method is more appealing owing to the following advantages. 1) It provides great flexibility for varying BF directions and power distribution between communication and sensing; 2) It enables constructive combining of communication and sensing subbeams at the communication receiver to improve the received signal power, especially when the two subbeams are overlapped.

In this paper, we study how to optimize the coefficient φ for a given ρ. We first derive the unconstrained optimal solution that maximizes the received signal power and signal-to-noise power ratio (SNR), without considering constraints on the scanning waveform. We then extend the results to the scenario when constraints are taken into account.

III. Optimization of φ without Constraints on Scanning Waveform

Assuming that the channel matrix $\mathbf{H}$ is known at the transmitter, we study how to optimize the phase parameter φ for any given ρ, $\mathbf{w}_{t,c}$ and $\mathbf{w}_{t,s}$. For $\mathbf{w}_r$, we assume that maximal ratio combining (MRC) [11] is applied at the receiver and $\mathbf{w}_r = (\mathbf{H}\mathbf{w}_t)^*$. The optimal φ, φ_{opt}, is obtained when the received signal power is maximized. The optimization problem can then be formulated as

$$\begin{aligned} \varphi_{\text{opt}} &= \arg\max_{\varphi} \frac{\mathbf{w}_t^H \mathbf{H}^H \mathbf{H} \mathbf{w}_t}{|\mathbf{w}_t|^2}, \\ &\text{with } \mathbf{w}_t = \sqrt{\rho}\mathbf{w}_{t,c} + \sqrt{1-\rho} e^{j\varphi} \mathbf{w}_{t,s}. \end{aligned} \tag{5}$$

Let $g_1(\varphi) = \mathbf{w}_t^H \mathbf{H}^H \mathbf{H} \mathbf{w}_t$ and $g_2(\varphi) = |\mathbf{w}_t|^2$. (5) can be rewritten as

$$\varphi_{\text{opt}} = \arg\max_{\varphi} \left(f(\varphi) \triangleq \frac{g_1(\varphi)}{g_2(\varphi)} \right), \text{ with} \tag{6}$$

$$\begin{aligned} g_1(\varphi) =& \rho \|\mathbf{H}\mathbf{w}_{t,c}\|^2 + (1-\rho)\|\mathbf{H}\mathbf{w}_{t,s}\|^2 \\ &+ P e^{j\varphi} \mathbf{w}_{t,c}^H \mathbf{H}^H \mathbf{H} \mathbf{w}_{t,s} + P e^{-j\varphi} \mathbf{w}_{t,s}^H \mathbf{H}^H \mathbf{H} \mathbf{w}_{t,c}, \\ g_2(\varphi) =& \rho \|\mathbf{w}_{t,c}\|^2 + (1-\rho)\|\mathbf{w}_{t,s}\|^2 + P e^{j\varphi} \mathbf{w}_{t,c}^H \mathbf{w}_{t,s} \\ &+ P e^{-j\varphi} \mathbf{w}_{t,s}^H \mathbf{w}_{t,c}, \end{aligned} \tag{7}$$

where $P \triangleq \sqrt{\rho(1-\rho)}$.

Next, we try to find its maximum by studying the monotonicity of $f(\varphi)$ and computing its derivatives. The first-order derivative of $f(\varphi)$ with respect to φ is given by

$$f'(\varphi) = \frac{g_1'(\varphi) g_2(\varphi) - g_2'(\varphi) g_1(\varphi)}{g_2(\varphi)^2} \tag{8}$$

Obviously, $g_2^2(\varphi) > 0$. Let the numerator in (8) be $h(\varphi)$, and let $\mathbf{w}_{t,c}^H \mathbf{H}^H \mathbf{H} \mathbf{w}_{t,s} = a_1 e^{j\alpha_1}$ and $\mathbf{w}_{t,c}^H \mathbf{w}_{t,s} = a_2 e^{j\alpha_2}$, where $a_1 \geq 0$ and $a_2 \geq 0$. We have

$$\begin{aligned} h(\varphi) =& -2Pa_1 \sin(\varphi + \alpha_1) - 4P^2 a_1 a_2 \sin(\alpha_1 - \alpha_2) + \\ & 2Pa_2[\rho \|\mathbf{H}\mathbf{w}_{t,c}\|^2 + (1-\rho)\|\mathbf{H}\mathbf{w}_{t,s}\|^2] \sin(\varphi + \alpha_2) \\ =& X_1 \sin(\varphi) + X_2 \cos(\varphi) + L, \end{aligned}$$

where

$$\begin{aligned} X_1 \triangleq& 2P|a_1| \cos(\alpha_1) + \\ & 2P|a_2|[\rho \|\mathbf{H}\mathbf{w}_{t,c}\|^2 + (1-\rho)\|\mathbf{H}\mathbf{w}_{t,s}\|^2] \cos(\alpha_2), \\ X_2 \triangleq& -2P|a_1| \sin(\alpha_1) + \\ & 2P|a_2|[\rho \|\mathbf{H}\mathbf{w}_{t,c}\|^2 + (1-\rho)\|\mathbf{H}\mathbf{w}_{t,s}\|^2] \sin(\alpha_2), \\ L \triangleq& -4P^2 |a_1||a_2| \sin(\alpha_1 - \alpha_2). \end{aligned}$$

By considering the sign of X_1, $h(\varphi)$ can be represented as

$$h(\varphi) = \begin{cases} \sqrt{X_1^2 + X_2^2} \sin(\varphi + \gamma) + L, & \text{if } X_1 \geq 0 \\ -\sqrt{X_1^2 + X_2^2} \sin(\varphi + \gamma) + L, & \text{if } X_1 < 0, \end{cases}$$

where $\gamma = \arctan(X_2/X_1)$.

Since $h(\varphi)$ is a periodic function and the period is 2π, we study the monotonicity of $f(\varphi)$ in one period. During a period of length π, $f(\varphi)$ keeps increasing if $h(\varphi) > 0$, and keeps decreasing otherwise. So at the transition point where $h(\varphi) = 0$, we can obtain either the maximum or minimum of $f(\varphi)$. From $h(\varphi) = 0$, we can get

$$\varphi = \begin{cases} -\mu_0 - \gamma, & \text{if } X_1 \geq 0 \\ \mu_0 - \gamma, & \text{if } X_1 < 0, \end{cases} \tag{9}$$

where $\mu_0 = \arcsin\left(\frac{L}{\sqrt{X_1^2 + X_2^2}}\right)$. To make sure that μ_0 exists, $|L| \leq \sqrt{X_1^2 + X_2^2}$ needs to be satisfied. This can be verified by proving that $L^2 \leq X_1^2 + X_2^2$, which is straightforward and omitted here due to page limit.

By analyzing the monotonic intervals of $h(\varphi)$, the maximum of $f(\varphi)$ can then be found as

$$\varphi_{\text{opt}} = \begin{cases} \pi + \mu_0 - \gamma + 2l\pi, & \text{if } X_1 \geq 0, \\ \mu_0 - \gamma + 2l\pi, & \text{if } X_1 < 0, \end{cases} \quad l = 0, \pm 1, \pm 2 \cdots \tag{10}$$

The complexity of calculating φ_{opt} is $O(M^2)$.

IV. Optimal Solutions with Constraints on Scanning Waveform

The combined BF waveform varies with different values of the combining coefficient φ. When it is optimized for maximizing the received signal power in Section III, the waveform at sensing directions may become distorted. In this section, we consider the optimization of φ under two types of constraints on the sensing subbeam.

A. Constrained BF Gain at Discrete Scanning Directions

We consider the cases where there are constraints on the minimum BF gain at several sensing directions. The thresholds of these minimum gains do not have a direct impact on our solutions. Here, we set the i-th threshold as $C_{s_i}^2(1-\rho)M$, where C_{s_i} is a scaling coefficient, and M represents the maximum gain that the array can achieve. With the minimum required gain at the i-th direction θ_{s_i}, we can formulate the constrained optimization problem as

$$\bar{\varphi}_{\text{opt}} = \arg\max_{\varphi} \frac{\mathbf{w}_t^H \mathbf{H}^H \mathbf{H} \mathbf{w}_t}{|\mathbf{w}_t|^2}, \tag{11a}$$

$$s.t. \ \frac{|\mathbf{a}^T(\theta_{s_i})\mathbf{w}_t|^2}{||\mathbf{w}_t||^2} \geq C_{s_i}^2(1-\rho)M, \ i = 1, 2, \cdots, N_s \tag{11b}$$

where N_s is the number total constraints, and C_{s_i} may take typical values from 0 to 1.

To solve this optimization problem, we first decide the range of φ that satisfies each of the constraints in (11b). Expanding the left-hand side of the i-th inequality in (11b), we get

$$\begin{aligned} |\mathbf{a}^T(\theta_{s_i})\mathbf{w}_t|^2 =& \rho |\mathbf{w}_{t,c}^H \mathbf{a}(\theta_{s_i})^*|^2 + (1-\rho)|\mathbf{w}_{t,s}^H \mathbf{a}(\theta_{s_i})^*|^2 \\ & + 2P\Re\mathfrak{e}\{e^{j\varphi} \mathbf{w}_{t,c}^H \mathbf{a}^*(\theta_{s_i}) \mathbf{a}(\theta_{s_i})^T \mathbf{w}_{t,s}\}, \\ ||\mathbf{w}_t||^2 =& \rho \|\mathbf{w}_{t,c}\|^2 + (1-\rho)\|\mathbf{w}_{t,s}\|^2 + 2P\Re\mathfrak{e}\{e^{j\varphi} \mathbf{w}_{t,c}^H \mathbf{w}_{t,s}\} \\ =& 1 + 2P\Re\mathfrak{e}\{e^{j\varphi} \mathbf{w}_{t,c}^H \mathbf{w}_{t,s}\}, \end{aligned} \tag{12}$$

where $P = \sqrt{\rho(1-\rho)}$. Let $\mathbf{w}_{t,c}^H \mathbf{w}_{t,s} = b_1 e^{j\beta_1}$, $\mathbf{w}_{t,c}^H \mathbf{a}(\theta_{s_i}) = b_{2i} e^{j\beta_{2i}}$, $\mathbf{a}(\theta_{s_i})^T \mathbf{w}_{t,s} = b_{3i} e^{j\beta_{3i}}$, $B_{1i} = \rho b_{2i}^2 + (1-\rho) b_{3i}^2$, and $B_{2i} = M C_{s_i}^2 (1-\rho)$, the inequality (11b) can be converted to

$$\begin{aligned} & C_{1i} \sin\varphi + C_{2i} \cos\varphi \geq \frac{B_{2i} - B_{1i}}{2P}, \\ & C_{1i} = b_1 B_{2i} \sin\beta_1 - b_{2i} b_{3i} \sin(\beta_{2i} + \beta_{3i}), \\ & C_{2i} = b_{2i} b_{3i} \cos(\beta_{2i} + \beta_{3i}) - b_1 B_{2i} \cos\beta_1. \end{aligned} \tag{13}$$

When $|B_{2i} - B_{1i}| \leq \sqrt{C_{1i}^2 + C_{2i}^2}$, we can get the solution to (13) as a set denoted by $\varphi \in \mathbb{k}_i = [\varphi_{1i}, \varphi_{2i}]$, where φ_{1i} and φ_{2i} denote the two bounds of the set. The set is given by

$$\begin{aligned} \mathbb{k}_i =& [\varphi_{1i}, \varphi_{2i}] \\ =& \begin{cases} [\mu_i - \sigma_i, -\mu_i + \pi - \sigma_i], & \text{if } C_{1i} \geq 0, \\ [\mu_i + \pi - \sigma_i, -\mu_i + 2\pi - \sigma_i], & \text{if } C_{1i} < 0, \end{cases} \end{aligned} \tag{14}$$

where $\mu_i = \arcsin\left(\frac{B_{2i} - B_{1i}}{\sqrt{C_{1i}^2 + C_{2i}^2}}\right) + 2k\pi, k = \pm 1, \pm 2, \cdots$, and $\sigma_i = \arctan\left(\frac{C_{2i}}{C_{1i}}\right)$.

When $B_{2i} - B_{1i} \leq -\sqrt{C_{1i}^2 + C_{2i}^2}$, we have $\mathbb{k}_i = \mathbf{R}$, i.e., any φ satisfies (12).

When $B_{2i} - B_{1i} \geq \sqrt{C_{1i}^2 + C_{2i}^2}$, we have $\mathbb{k}_i \in \varnothing$, i.e., no φ satisfies (12) at the required ratio C_{s_i}. This should be avoided by carefully setting the values of C_{s_i}. After obtaining the sets for all inequality constraints, we can derive the final range of φ by finding their intersection as

$$\begin{aligned} \varphi \in \mathcal{K} \triangleq& \{\mathbb{k}_1 \cap \mathbb{k}_2 \cap \cdots \cap \mathbb{k}_{N_s}\} \\ =& \{[\varphi_{11}, \varphi_{21}] \cap [\varphi_{12}, \varphi_{22}] \cap \cdots \cap [\varphi_{1N_s}, \varphi_{2N_s}]\} \\ =& \begin{cases} [\varphi_{s1}, \varphi_{s2}], & \text{if } \varphi_{s1} \leq \varphi_{s2}, \\ \varnothing, & \text{otherwise,} \end{cases} \end{aligned} \tag{15}$$

where $\varphi_{s1} = \max\{\varphi_{11}, \varphi_{12}, \cdots, \varphi_{1N_s}\}$, and $\varphi_{s2} = \min\{\varphi_{21}, \varphi_{22}, \cdots, \varphi_{2N_s}\}$.

It is worth noting that generally, the range of φ decreases with the increase of N_s. For a specific constraint $\frac{|\mathbf{a}^T(\theta_{s_i})\mathbf{w}_t|}{||\mathbf{w}_t||} \geq C_{s_i}\sqrt{1-\rho}M$, reducing the value of C_{s_i} can relax the restrictions of φ, while reducing the gain in the direction θ_s. Thus, the values of N_s and C_{s_i} can affect the effectiveness of these constraints. If $\mathcal{K}$ exists, by comparing φ_{opt} obtained by (10) and $\mathcal{K}$, the φ_{opt} can be found as

$$\bar{\varphi}_{\text{opt}} = \begin{cases} \varphi_{\text{opt}}, & \text{if } \varphi_{\text{opt}} \in \mathcal{K}, \\ \varphi_{s1}, & \text{if } \varphi_{\text{opt}} \notin \mathcal{K} \text{ and } \Delta_{\text{min1}} \leq \Delta_{\text{min2}}, \\ \varphi_{s2}, & \text{if } \varphi_{\text{opt}} \notin \mathcal{K} \text{ and } \Delta_{\text{min1}} > \Delta_{\text{min2}} \end{cases} \tag{16}$$

where $\Delta_{\text{min1}} = \min\{|\varphi_{s1} - \varphi_{\text{opt}}|\}$, and $\Delta_{\text{min2}} = \min\{|\varphi_{s2} - \varphi_{\text{opt}}|\}$.

Since φ_{opt} is obtained at the maximum of a sine function of period 2π and the length of the range $[\varphi_{1i}, \varphi_{2i}]$ is π, (16) actually finds the value of φ that is the closest to φ_{opt}, i.e., the φ that achieves the maximal received signal power satisfying (15). The additional complexity of calculating $\bar{\varphi}_{\text{opt}}$ is bounded by $O(M^2)$, since usually $N_s \leq M$.

When a single constraint on the desired scanning direction that $\mathbf{w}_{t,s}$ points to, a relatively simple yet practical solution can be obtained without looking into complicated computation of the intersection.

B. Constrained Total Scanning Power over a Range of Directions

As we have shown in Section IV-A, finding the solution for φ to meet the gain constraints on multiple discrete directions can be complicated when the number of constraints is large. It is not always possible to find the optimal solution unless the intersection exists. In practice, it could be more common to require a minimum total power constraint over a range of consecutive scanning directions, for example, within the 3dB beamwidth. In this section, we investigate the optimization problem under such a minimum total power constraint. The problem can be formulated as

$$\hat{\varphi}_{\text{opt}} = \arg\max_{\varphi} \frac{\mathbf{w}_t^H \mathbf{H}^H \mathbf{H} \mathbf{w}_t}{|\mathbf{w}_t|^2}, \tag{17a}$$

$$\text{s.t.} \int_{\theta_{s_1}}^{\theta_{s_2}} \frac{|\mathbf{a}^T(\theta)\mathbf{w}_t|^2}{||\mathbf{w}_t||^2} d\theta \geq C_{sp} \int_{\theta_{s_1}}^{\theta_{s_2}} |\mathbf{a}^T(\theta)\mathbf{w}_2|^2 d\theta, \tag{17b}$$

where θ_{s_1} and θ_{s_2} are the bounds of the BF range of interest, C_{sp} is a scaling coefficient, and $\mathbf{w}_2$ is the BF weight used in Method 2 in [4]. Once again, the threshold does not have a direct impact on our solution. The one we use here is to refer the constraint to the BF gain achieved by the joint BF design method in [4].

Note that the integration is with respect to θ and unrelated to $\mathbf{w}_t$, we can take $\mathbf{w}_t$ out of the integration. For example, we can have

$$\int_{\theta_{s_1}}^{\theta_{s_2}} \frac{|\mathbf{a}^T(\theta)\mathbf{w}_t|^2}{||\mathbf{w}_t||^2} d\theta = \frac{\mathbf{w}_t^H \left(\int_{\theta_{s_1}}^{\theta_{s_2}} \mathbf{a}^*(\theta)\mathbf{a}^T(\theta) d\theta \right) \mathbf{w}_t}{||\mathbf{w}_t||^2}. \tag{18}$$

Let $\mathbf{A}(\theta) = \mathbf{a}^*(\theta)\mathbf{a}^T(\theta)$. We cannot obtain an explicit result for the integral of each element in $\mathbf{A}(\theta)$. We can instead approximate the integral as a summation, as follows

$$\boldsymbol{\mathcal{A}} = \int_{\theta_{s_1}}^{\theta_{s_2}} \mathbf{A}(\theta) d\theta \approx \sum_{i=1}^{N_I} \delta_\theta \mathbf{A}(\theta_{s_1} + i\delta_\theta). \tag{19}$$

where $\delta_\theta = (\theta_{s_2} - \theta_{s_1})/N_I$ is the step size and N_I is the total steps. It is assumed that N_I is large enough to guarantee a small enough step size. For a set of values of θ_{s_1} and θ_{s_2}, we can pre-calculate and store the numerical results. Since $\mathbf{A}$ is a Toeplitz matrix, only $(2M-1)$ numerical integrations are to be calculated and stored for a given range of sensing BF directions. The complexity of calculating $\boldsymbol{\mathcal{A}}$ is $O(MN_I)$.

Once the integration is available, we can proceed to solve the optimization problem. Similar to the derivation process in Section IV-A, (17b) can be written as

$$\begin{aligned} \frac{h_{p_1}(\varphi)}{h_{p_2}(\varphi)} \geq & C_{sp}\mathbf{w}_2^H \boldsymbol{\mathcal{A}} \mathbf{w}_2 \text{ (or } C_{sp_2}\mathbf{w}_s^H \boldsymbol{\mathcal{A}} \mathbf{w}_s), \text{ where} \\ h_{p_1}(\varphi) = & \rho \mathbf{w}_{t,c}^H \boldsymbol{\mathcal{A}} \mathbf{w}_{t,c} + (1-\rho)\mathbf{w}_{t,s}^H \boldsymbol{\mathcal{A}} \mathbf{w}_{t,s} \\ & + 2P\mathfrak{Re}\{e^{j\varphi}\mathbf{w}_{t,c}^H \boldsymbol{\mathcal{A}} \mathbf{w}_{t,s}\}, \\ h_{p_2}(\varphi) = & \rho\|\mathbf{w}_{t,c}\|^2 + (1-\rho)\|\mathbf{w}_{t,s}\|^2 + 2P\mathfrak{Re}\{e^{j\varphi}\mathbf{w}_{t,c}^H \mathbf{w}_{t,s}\} \\ = & 1 + 2P\mathfrak{Re}\{e^{j\varphi}\mathbf{w}_{t,c}^H \mathbf{w}_{t,s}\}. \end{aligned} \tag{20}$$

Let $\mathbf{w}_{t,c}^H \boldsymbol{\mathcal{A}} \mathbf{w}_{t,s} = b_p e^{j\beta_p}$, $B_{p_1} = \rho \mathbf{w}_{t,c}^H \boldsymbol{\mathcal{A}} \mathbf{w}_{t,c} + (1-\rho)\mathbf{w}_{t,s}^H \boldsymbol{\mathcal{A}} \mathbf{w}_{t,s}$, and $B_{p_2} = C_{sp}\mathbf{w}_2^H \boldsymbol{\mathcal{A}} \mathbf{w}_2$, (20) can be converted to

$$\begin{aligned} & C_{p_1}\sin\varphi + C_{p_2}\cos\varphi \geq \frac{B_{p_2} - B_{p_1}}{2P}, \text{where} \\ & C_{p_1} = b_1 B_{p_2}\sin\beta_1 - b_p\sin(\beta_p), \\ & C_{p_2} = b_p\cos(\beta_p) - b_1 B_{p_2}\cos\beta_1. \end{aligned} \tag{21}$$

For $|B_{p_2} - B_{p_1}| \leq \sqrt{C_{p_1}^2 + C_{p_2}^2}$, we can obtain

$$\begin{aligned} \varphi \in \mathbb{k}_p &= [\varphi_{p1}, \varphi_{p2}] \\ &= \begin{cases} [\mu_p - \sigma_p, -\mu_p + \pi - \sigma_p], & \text{if } C_{p_1} \geq 0, \\ [\mu_p + \pi - \sigma_p, -\mu_p + 2\pi - \sigma_p], & \text{if } C_{p_1} < 0, \end{cases} \end{aligned} \tag{22}$$

where $\mu_p = \arcsin(\frac{B_{p_2} - B_{p_1}}{\sqrt{C_{p_1}^2 + C_{p_2}^2}}) + 2k\pi$, $k = \pm 1, \pm 2, \cdots$ and $\sigma_p = \arctan(\frac{C_{p_2}}{C_{p_1}})$.

When $B_{p_2} - B_{p_1} \leq -\sqrt{C_{p_1}^2 + C_{p_2}^2}$, we have $\mathbb{k}_p = \mathbf{R}$. When $B_{p_2} - B_{p_1} > \sqrt{C_{p_1}^2 + C_{p_2}^2}$, we have $\mathbb{k}_p \in \varnothing$. By setting proper C_{sp}, it can be generally guaranteed that $\mathbb{k}_p \notin \varnothing$. Therefore, $\hat{\varphi}_{\text{opt}}$ under constrained total power can be obtained as

$$\hat{\varphi}_{\text{opt}} = \begin{cases} \varphi_{\text{opt}}, & \text{if } \varphi_{\text{opt}} \in \mathbb{k}_p, \\ \varphi_{p1}, & \text{if } \varphi_{\text{opt}} \notin \mathbb{k}_p \text{ and } \Delta_{p1} \leq \Delta_{\text{min2}}, \\ \varphi_{p2}, & \text{if } \varphi_{\text{opt}} \notin \mathbb{k}_p \text{ and } \Delta_{p1} > \Delta_{\text{min2}} \end{cases} \tag{23}$$

$\Delta_{p1} = \min\{|\varphi_{p1} - \varphi_{\text{opt}}|\}, \Delta_{p2} = \min\{|\varphi_{p2} - \varphi_{\text{opt}}|\}$.

The complexity of calculating $\tilde{\varphi}_{\text{opt}}$ is $O(M^2)$ if $M \geq N_I$, or $O(MN_I)$ otherwise.

V. Simulation Results

In this section, simulation results are presented to verify the proposed optimal combining coefficients. For all simulations, a ULA with $M = 16$ omnidirectional antennas (spaced at half wavelength) is used. We assume that the basic reference beam for communication and sensing are pointed at zero degree. The 3dB beamwidth for a linear array with K_s antennas is approximately $2\arcsin(\frac{1.2}{K_s})$ in radii. We generate the basic beams with $K_s = 16$ and $K_s = 12$ for the communication and sensing subbeams, respectively. The power distribution factor ρ is set as 0.5. For Figs. 1 and 2, the results are averaged over 500 realizations.

In the simulation, $\mathbf{w}_{t,c}$ is set as the conjugate of $\mathbf{a}(\theta_t)$, where θ_t is the dominating AoD. $\mathbf{w}_{t,s}$ is generated by multiplying a phase-shifting sequence to the basic sensing subbeam to change the pointing directions, as described in [4]. For all results on the received signal power, an MRC receiver is assumed to be used, and they are normalized to the power value when the whole transmitter array generates a single beam pointing to the dominating AoD. In the legends of all the figures, the first and second methods in [4] are denoted as "M1-Zhang19" and "M2-Zhang19" respectively. "Maximal Rx Power", "Constrain gain", and "Constrain power" denote the three proposed BF methods introduced in Sections III, IV-A and IV-B, respectively.

In Figs. 1 and 2, we show the normalized received signal power and MSE of waveform change for several methods. For comparison, we also display the BF results when no phase shifting term is used (denoted as "Without phase shifting"). The case where scanning directions are close to communication is studied. In Fig. 1, we can see that when the communication and sensing subbeams overlap considerably, the optimized phase shifting terms lead to higher received signal power, compared to the methods in [4]. Without considering the sensing performance, "Maximal Rx Power" achieves the largest output power, as expected. It is shown in Fig. 2 that the methods with constraints can generally achieve an MSE closer to Method 2 in [4]. By summing up the mismatches at all directions, the MSE can only reflect the overall waveform characteristics. More detailed results illustrating the waveform difference are displayed in the following BF radiation patterns.

In Fig. 3, we present the multibeam BF radiation pattern generated by Method 1 and Method 2 in [4], and the three proposed methods in this paper. From the figure, we can see that there can be a gain degradation at the desired scanning directions when no constraints are applied in the optimization. With constraints considered, a BF waveform close to the one using Method 2 in [4] is achieved.

Fig. 4 displays an example of the influence of C_s on the BF radiation pattern. Although only the minimum gain at one direction is applied, the gain within the whole 3dB beamwidth is correspondingly improved. We can also observe that increasing C_s can effectively improve the gain of the sensing subbeam up to an upper limit. Similar results can also be observed with the change of C_{sp} in (17b) (not shown here due to page limit).

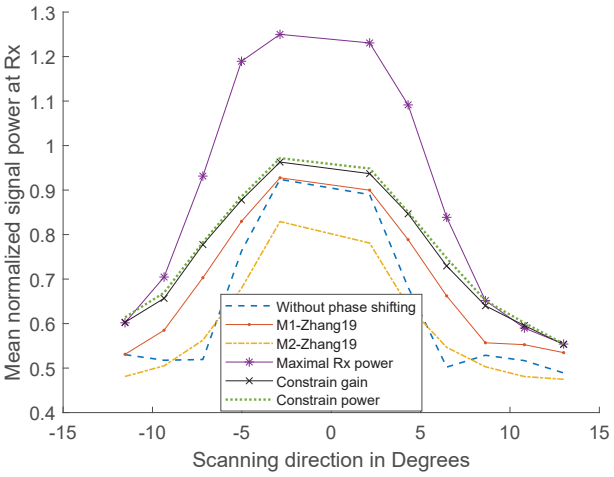

Fig. 1. Averaged normalized received signal power for different combining coefficients when the sensing subbeam points to various directions. For the cases with constraints, $C_s = C_{sp} = 0.9$.

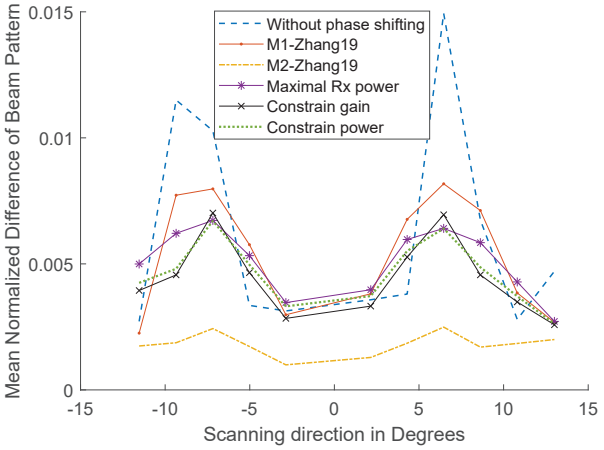

Fig. 2. Averaged normalized MSE of waveform for different combining coefficients when the sensing subbeam points to various directions. For the cases with constraints, $C_s = C_{sp} = 0.9$.

With constraints on the total scanning power, Fig. 5 plots the BF radiation pattern obtained by different ranges $(\theta_{s2} - \theta_{s1})$. We can see that a wider scanning BF range can lead to a lower scanning power in the desired central scanning direction, since the total power is constrained. In our simulations, it is observed that when $N_I \geq 12$, each element in $\boldsymbol{\mathcal{A}}$ can achieve errors less than 10^{-3} compared to the convergence limits, and the BF radiation pattern achieved by these values are nearly identical.

VI. Conclusions

We have studied the optimization of the coefficient for combining communication and sensing BF vectors in a multibeam JCAS system. When the full channel knowledge is known, closed-form expressions for the optimal combining coefficient that maximize the received signal power were provided, in the

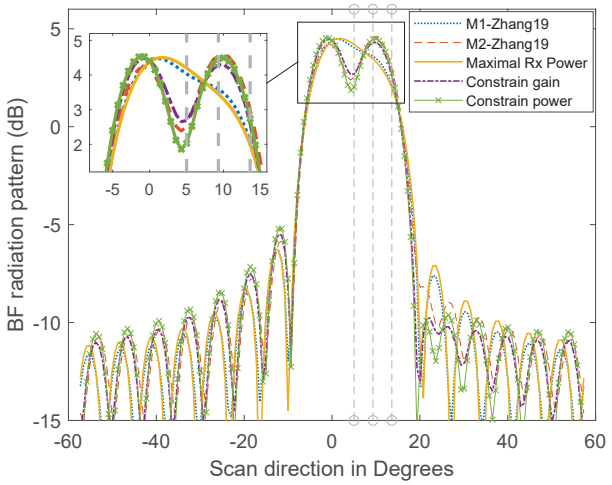

Fig. 3. BF radiation pattern for several methods when $C_s = C_{sp} = 0.9$, and integral range $(\theta_{s2} - \theta_{s1})$ is $1.43°$. The desired dominant scanning direction and the 3dB beamwidth are marked by grey dash.

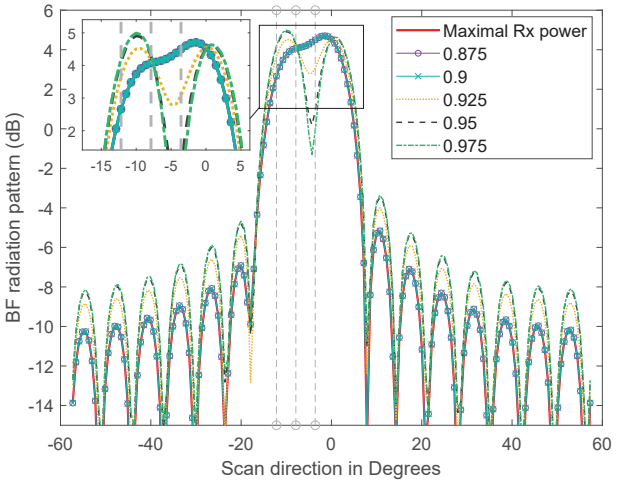

Fig. 4. BF radiation pattern generated by different values of C_s, which vary from 0.875 to 0.975, when the scanning subbeam points to $-9.31°$. The desired dominant scanning direction and the 3dB beamwidth are marked by grey dash.

cases with and without constraints on the sensing BF waveform. Simulation results verify that these optimal solutions perform efficiently in balancing the received signal power for communication and the scanning BF waveform for sensing. The proposed methods have low complexity and can adapt rapidly to time-varying channels.

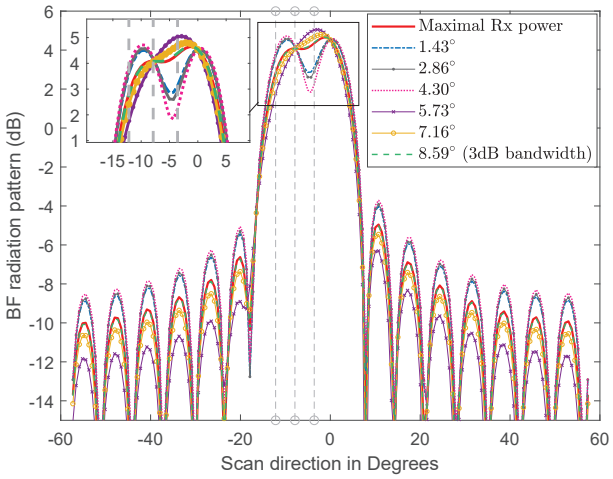

Fig. 5. BF radiation pattern generated by different integral range $(\theta_{s2} - \theta_{s1})$, from the 3dB beamwidth of the scanning beam $8.59°$ to $1.43°$, centered at $-9.31°$, the dominant AoD of the scanning beam. The desired dominant scanning direction and the 3dB beamwidth are marked by grey dash.

REFERENCES

[1] C. Sturm and W. Wiesbeck, "Waveform design and signal processing aspects for fusion of wireless communications and radar sensing," *Proc. IEEE*, vol. 99, no. 7, pp. 1236–1259, 2011.

[2] L. Han and K. Wu, "Joint wireless communication and radar sensing systems–state of the art and future prospects," *IET Microw. Antennas Propag.*, vol. 7, no. 11, pp. 876–885, 2013.

[3] N. González-Prelcic, R. Méndez-Rial, and R. W. Heath, "Radar aided beam alignment in mmWave V2I communications supporting antenna diversity," in *Inform. Theory Appl. Workshop (ITA), 2016*. IEEE, 2016, pp. 1–7.

[4] J. A. Zhang, X. Huang, Y. J. Guo, J. Yuan, and R. W. Heath, "Multibeam for joint communication and radar sensing using steerable analog antenna arrays," *IEEE Trans. Veh. Technol.*, vol. 68, no. 1, pp. 671–685, 2019.

[5] J. A. Zhang, X. Huang, V. Dyadyuk, and Y. J. Guo, "Massive hybrid antenna array for millimeter-wave cellular communications," *IEEE Wireless Commun. Mag.*, vol. 22, no. 1, pp. 79–87, 2015.

[6] L. Yan, X. Fang, H. Li, and C. Li, "An mmWave wireless communication and radar detection integrated network for railways," in *Veh. Technol. Conf. (VTC Spring), 2016 IEEE 83rd*. IEEE, 2016, pp. 1–5.

[7] V. Va and R. W. Heath, "Performance analysis of beam sweeping in millimeter wave assuming noise and imperfect antenna patterns," in *Veh. Technol. Conf. (VTC-Fall), 2016 IEEE 84th*. IEEE, 2016, pp. 1–5.

[8] P. Kumari, J. Choi, N. González-Prelcic, and R. W. Heath, "IEEE 802.11 ad-based radar: An approach to joint vehicular communication-radar system," *IEEE Trans. Veh. Technol.*, vol. 67, no. 4, pp. 3012–3027, 2018.

[9] X. Wang, A. Hassanien, and M. Amin, "Dual-function MIMO Radar communications system design via sparse array optimization," *IEEE Trans. on Aerospace and Electronic Systems*, vol. PP, pp. 1–1, 08 2018.

[10] F. Liu, L. Zhou, C. Masouros, A. Li, W. Luo, and A. Petropulu, "Toward dual-functional radar-communication systems: Optimal waveform design," vol. 66, no. 16, pp. 4264–4279, 2018.

[11] T. K. Lo, "Maximum ratio transmission," in *Commun., 1999. ICC'99. 1999 IEEE Int. Conf. on*, vol. 2. IEEE, 1999, pp. 1310–1314.